Supplemental Figures & Tables

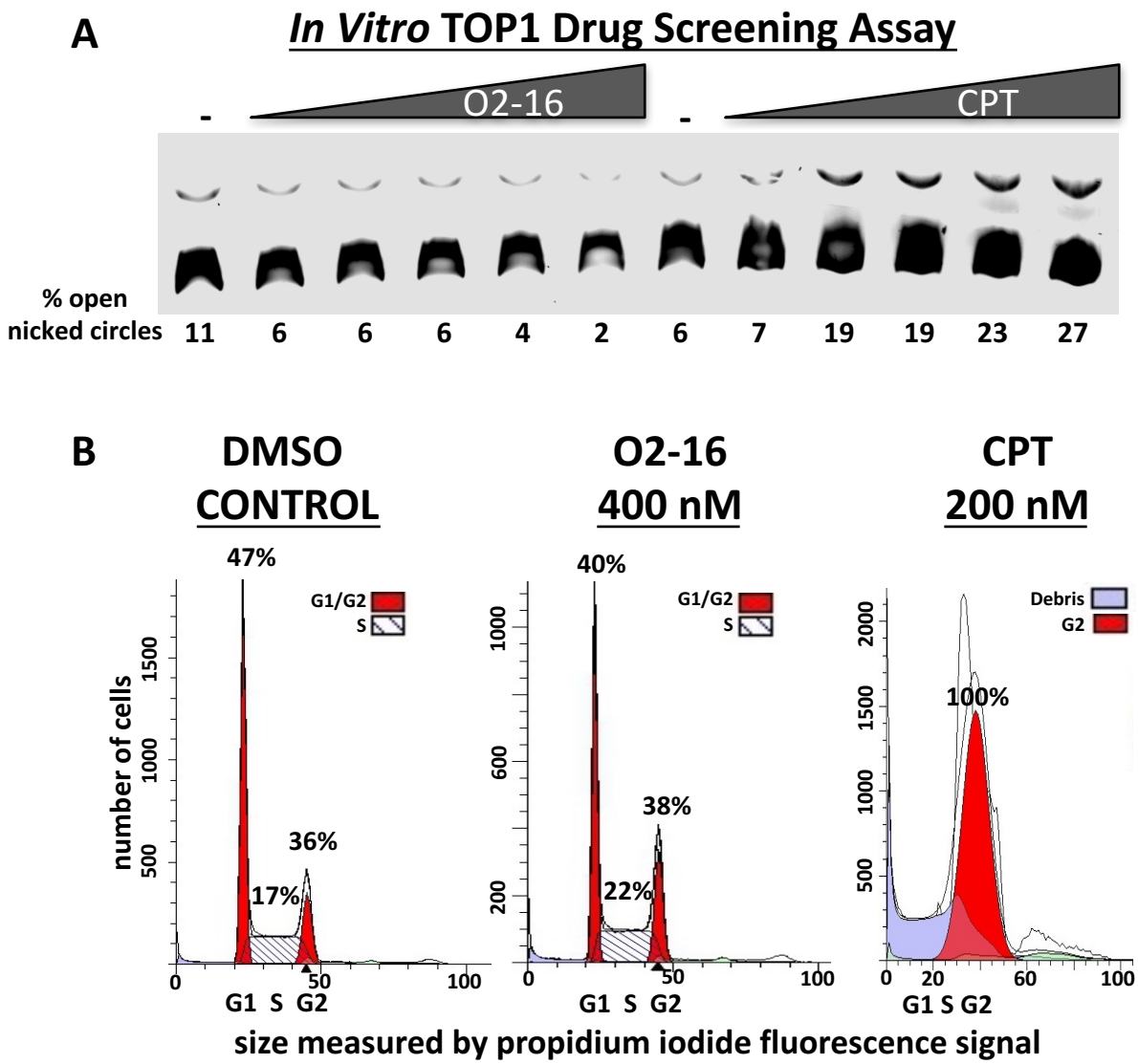

FIG. S1 related to FIG 1. TOP1 inhibitory activity of CPT, but not O2-16. (A) The *in vitro* TOP1 Drug Screening Assay (Topogen) performed according to manufacturer's protocol shows Ethidium Bromide stained plasmid DNA run on a 1% agarose gel treated with increasing amounts of O2-16 and CPT (50, 100, 250, 375, 500 µM) incubated with TOP1 enzyme. CPT is capable of trapping plasmid DNA into open nicked circles (top band) due to TOP1 inhibiting activity while the same concentrations of O2-16 showed no increase in open nicked circles compared to the (-) control (quantification of % open nicked circles by densitometry with Image J software is below the lanes). (B) A3.01 cells were treated with DMSO, 400 nM O2-16, or 200 nM CPT for 24 hours and fixed with 70% ethanol. Fixed cells were incubated with 1 mg/mL RNase A in PBS for 30 minutes followed by addition of 20 µg/mL of propidium iodide in PBS. The cells were then analyzed by Fluorescence-activated cell sorting (FACS) by the University of Rochester Flow Core. The data was run through Modfit software (Verity Software House) and the graphs show the number of cells in G1, S, and G2 with % of total in each phase listed above the peaks. 400 nM O2-16 had peak values similar to the DMSO control opposed to 200 nM CPT that had a large amount of cell debris and a 100% G2 block.

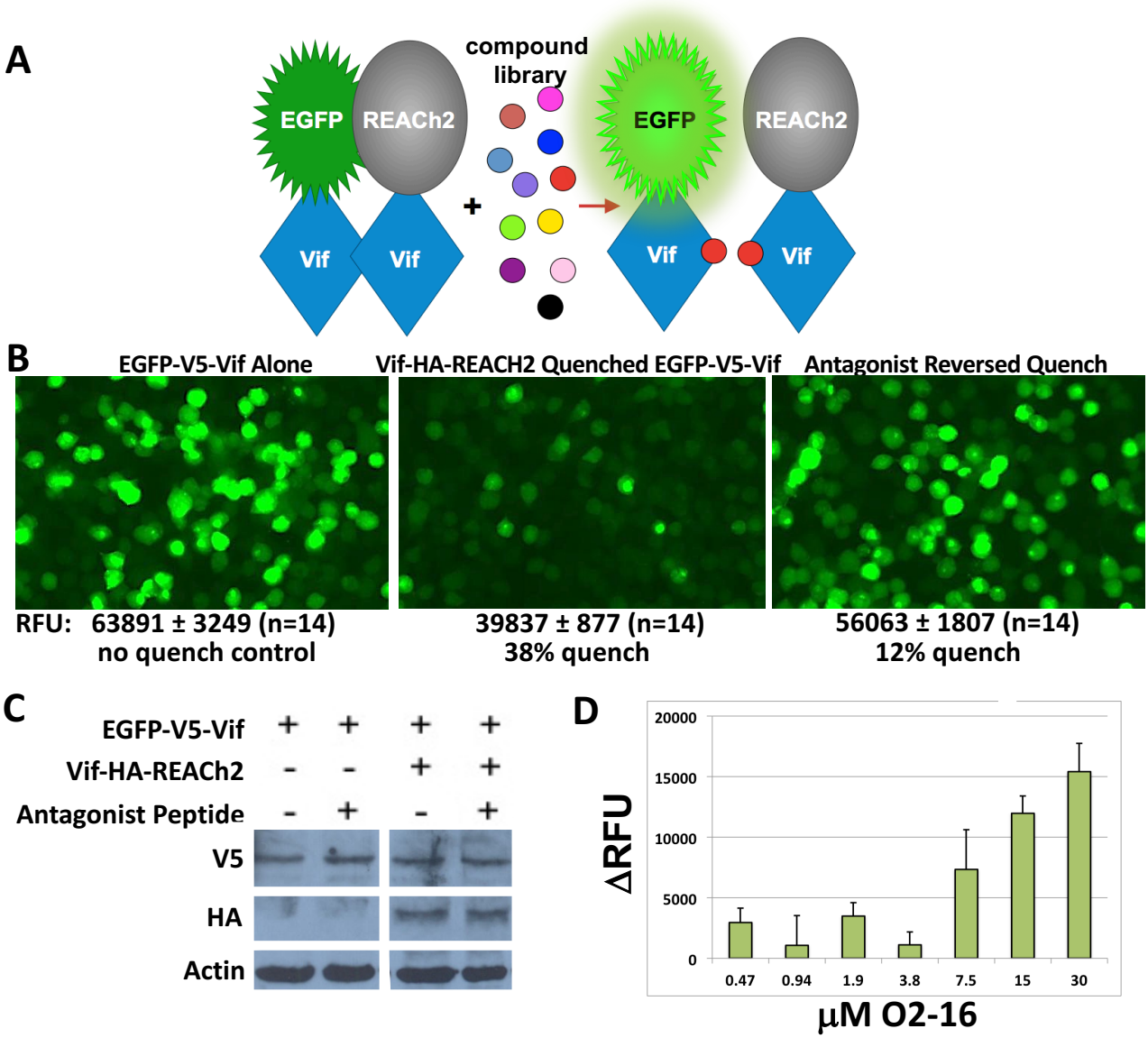

FIG. S2 related to FIG. 1B. In-cell FqRET Assay for Vif Multimerization. (A) A cartoon of the Vif multimerization assay showing that through an interaction between Vif molecules the donor EGFP is close to the acceptor REACh2 enabling fluorescence quenching, but in the presence of a compound that blocks Vif self-association, donor and acceptor are not close enough to quench and signal is increased. (B) The Vif multimerization assay was set up as in the Materials and Methods section. Fluorescence levels that were quantified in wells containing cells transfected with EGFP-chimera but not REACh2 (**left image**) or reversed by an 50 μM antagonist peptide (**right image**) were sufficiently greater than the quenched condition (**middle image**). The RFU obtained by the plate reader are shown below each image with SD for an n=14 along with the % quench. EGFP covalently bound to REACh2 through a cleavable linker quenches 50% and is maximum expected quench (Ganesan et al., 2006). Fluorescent images from an Olympus IX 81 using a FITC filter cube and a Hamamatsu ORCA-05G camera were false colored Green with Image J software (NIH). (C) Western blots show extracts from cells expressing V5 and HA epitope tagged Vif with Actin as a loading control for equivalent amount of cellular material and they reveal equivalent expression of EGFP-V5-Vif under conditions shown in (B) underscoring that the reduced fluorescence in the quenched condition was not due to lower protein expression but in fact a reflection of quenched signal. (D) O2-16 displays a dose-response (0.47-30 μM) in the change in relative fluorescence units (ΔRFU) in the screen. ΔRFU measures the difference between RFU before and 24 hours after compound addition with the DMSO control ΔRFU set to 0 with error bars showing SD (n=3) .

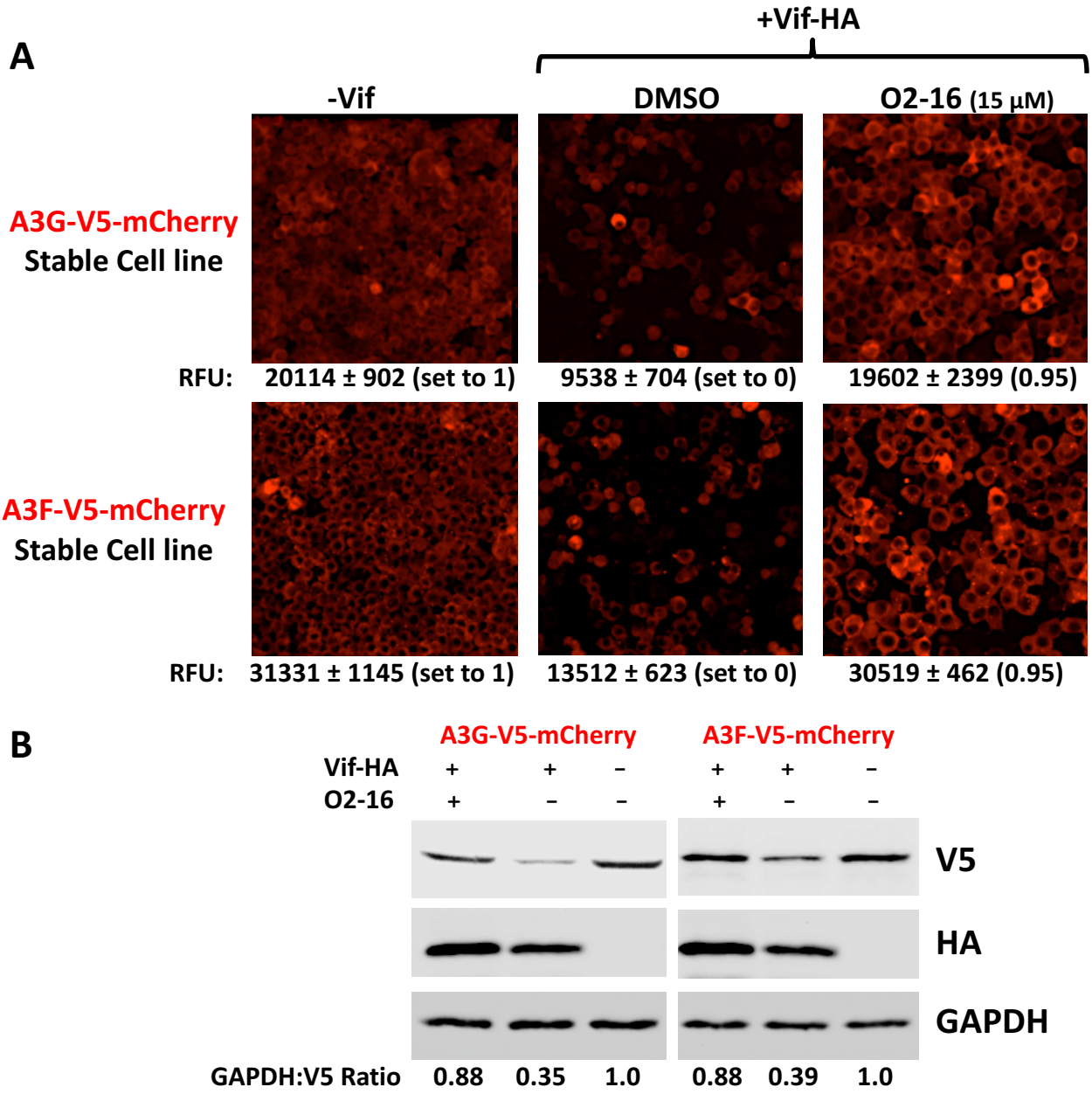

FIG. S3 related to FIG. 1C and 2A. Vif-Dependent A3G-mCherry and A3F-mCherry Degradation Assays. (A) A3G-V5-mCherry (top) and A3F-V5-mCherry (bottom) were stably expressed in 293T cells under puromycin selection. Fifty ng of subtype C Vif-HA was transiently transfected into the cells in 384-well format with Turbofect (Thermo). Four hours after transfection the compounds or DMSO were added to cells. Twenty-four hours after compound addition, the mCherry signal was read on a Biotek Synergy4 plate reader. The RFU from cells plated but not transfected with Vif were averaged and set at 1 (**left image**) with SD for an n=120 shown below the image. Cells transfected with Vif and treated only with DMSO were averaged and set at 0 RFU (**middle image**), average with SD for an n=5 is shown below the image. The **right image** shows that 15 µM prevented Vif-dependent A3G degradation, the RFU average with SD for an n=3 is shown below the image. Fluorescent images from an Olympus IX 81 using a Texas Red filter cube and a Hamamatsu ORCA-05G camera were false colored Red with Image J software (NIH). (B) Western blots for A3G-V5-mCherry (left) and A3F-V5-mCherry (right) cells, Vif-HA and GAPDH as a loading control show the loss of A3G and A3F protein when Vif was expressed and more protein abundance in the presence of 15 µM O2-16. The densitometric ratio of GAPDH:V5 is shown to quantify the abundance A3G and A3F when Vif and O2-16 are present compared to no O2-16 with and without Vif.

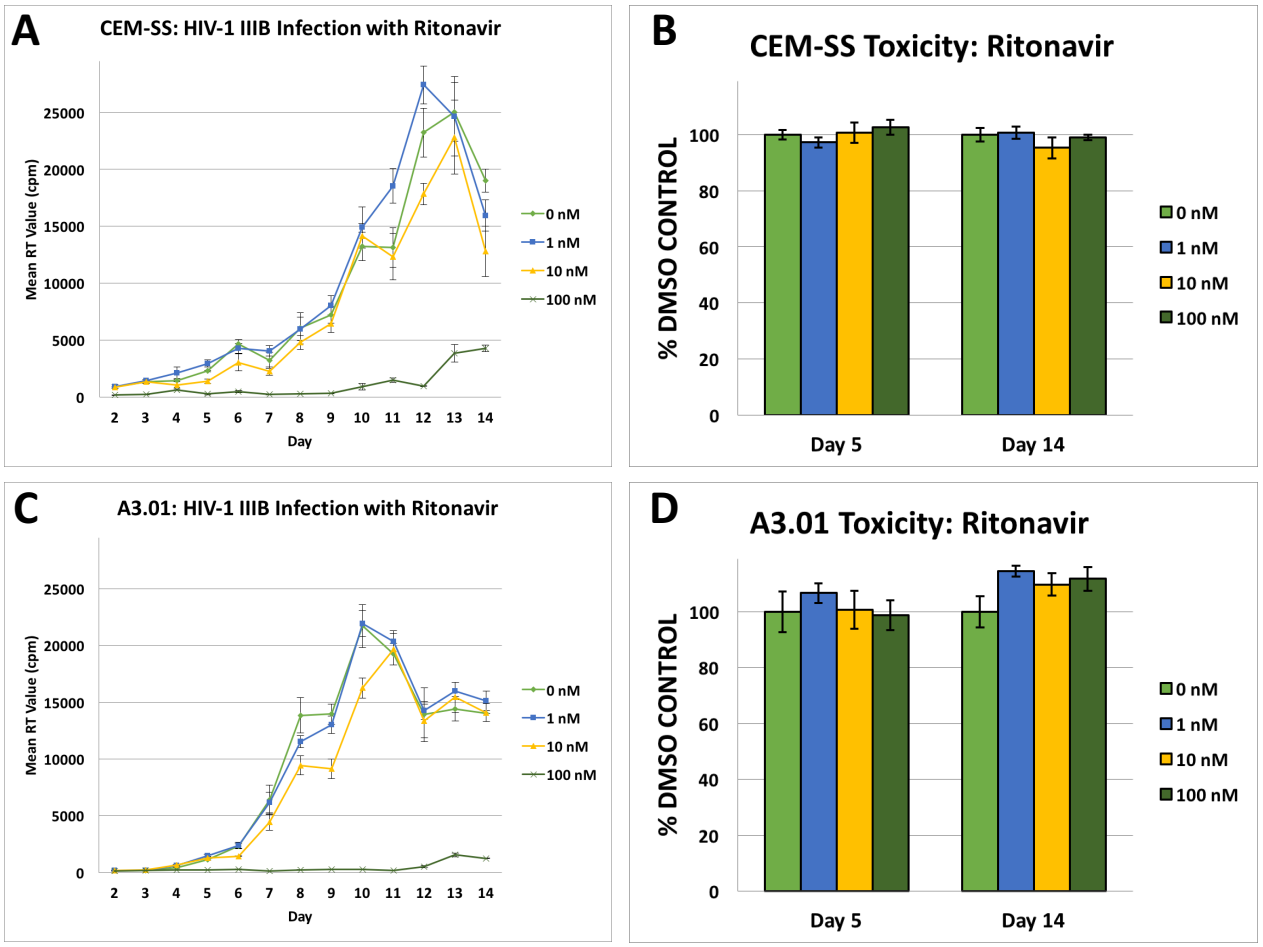

FIG. S4 related to FIG. 3. HIV Protease Inhibitor Ritonavir Antiviral Activity and Toxicity in CEM-SS and A3.01 cells. (A) CEM-SS and (C) A3.01 14-day HIV_{IIIB} infections at low MOI were treated every other day with 0, 1, 10, and 100 nM of HIV protease inhibitor Ritonavir. RT activity was measured with radioactive nucleotides and measured by radioactive counts per minute (cpm) to determine relative HIV abundance in the media. Ritonavir neutralized HIV in both cell types at 100 nM, n=3 with error bars showing SD values. (B) CEM-SS and (D) A3.01 cytotoxicity relative to DMSO control at days 5 and 14 measured by tetrazolium dye, n=3 with error bars showing SD.

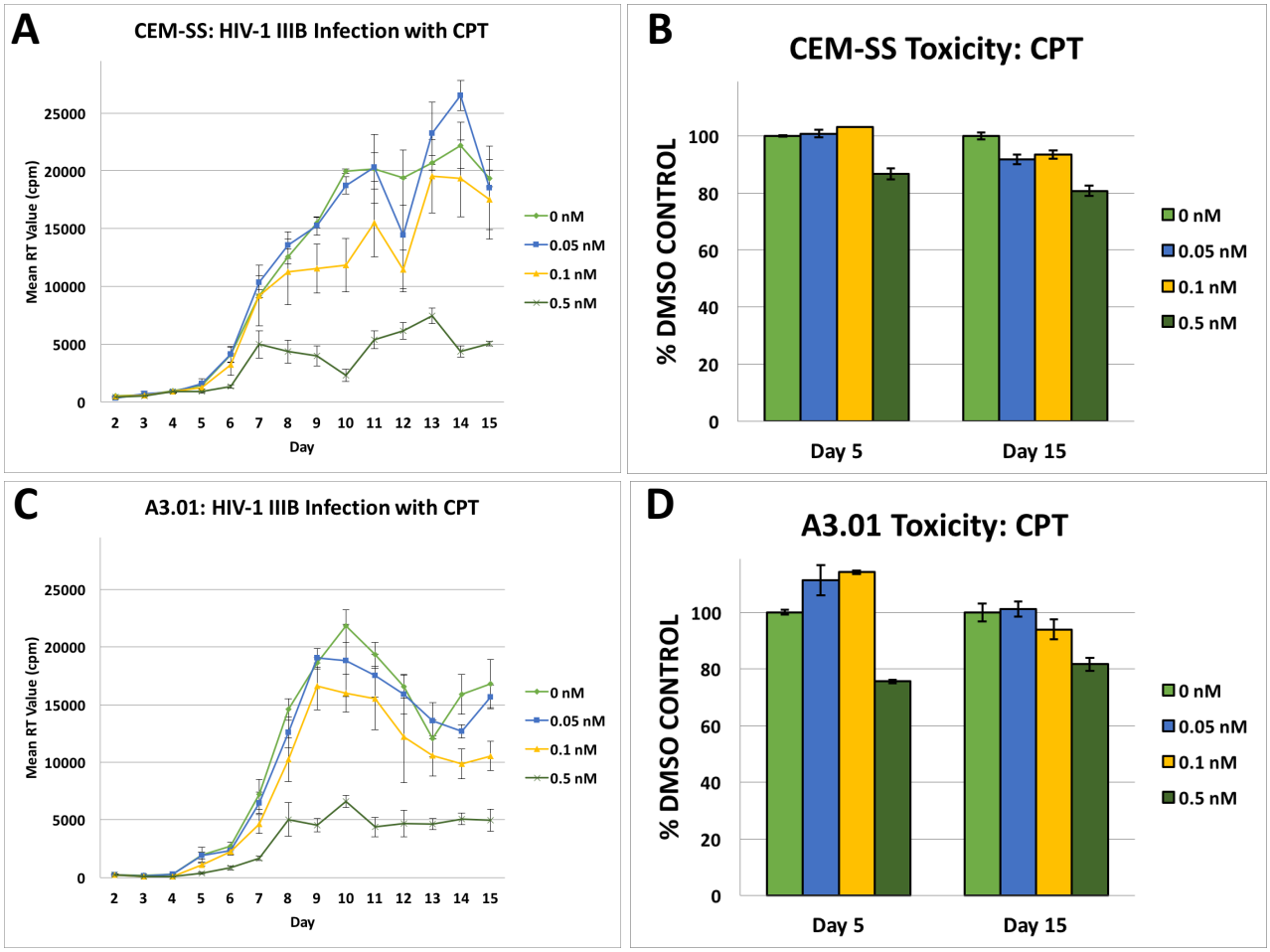

FIG. S5 related to FIG. 3. CPT Antiviral Activity and Toxicity in CEM-SS and A3.01 cells. (A) CEM-SS and (C) A3.01 15-day HIV_{IIIB} infections at low MOI were treated every other day with 0, 0.05, 0.1, and 0.5 nM of CPT. RT activity was measured with radioactive nucleotides and measured by radioactive counts per minute (cpm) to determine relative HIV abundance in the media. CPT inhibited HIV in both cell types at 0.5 nM, n=3 with error bars showing SD values. (B) CEM-SS and (D) A3.01 cytotoxicity relative to DMSO control at days 5 and 15 measured by tetrazolium dye, n=3 with error bars showing SD.

TABLE S1. *In Vitro* Toxicity Tests: O2-16

Test		Day				
Cytostasis	**Cell Type**	**1**	**2**	**3**		
Cell Count [a]	HepG2	-		+		
Cell Cycle Arrest [a]	HepG2	+		+		
Mitosis Marker (P-H3) [a]	HepG2	-		+/-		
Nuclear Size [a]	HepG2	+		+		
Morphology	**Cell Type**	**1**	**2**	**3**		
Cytoskeletal Disruption (Microtubules) [a]	HepG2	-		+/-		
Mitochondrial Mass [a]	HepG2	-		+		
Nuclear Size [a]	Rat Hepatocytes	-	-			
Stress and Apoptosis	**Cell Type**	**1**	**2**	**3**		
Stress Kinase Activation (c-jun) [a]	HepG2	-		+/-		
DNA Damage Response (p53) [a]	HepG2	+/-		+/-		
Oxidative Stress (H2AX) [a]	HepG2	+/-		+/-		
Mitochondrial Potential (TMRE) [a]	HepG2	-		-		
DNA Fragmentation [a]	Rat Hepatocytes	-	-			
ER stress/DNA Damage (Gadd153) [a]	Rat Hepatocytes	-	-			
Apoptosis (Cytochrome c) [a]	Rat Hepatocytes	-	-			
Phospholipidosis/Lysosomal mass (Lysotracker Red) [a]	Rat Hepatocytes	-	-			
Mitochondrial Potential (TMRE) [a]	Rat Hepatocytes	-	-			
Steatosis (LipidTox Far Red) [a]	Rat Hepatocytes	-	-			
ROS [a]	Rat Hepatocytes	-				
Glutathione [a]	Rat Hepatocytes	-				
APO-ONE Homogeneous Caspase-3/7 [b]	HeLa			-		
CytoTox-ONE Homogeneous Membrane Integrity [b]	HeLa			-		
Viability	**Cell Type**	**1**		**3**	**5**	**14**
XTT Assay [b]	Unstimulated PBMCs			-		
XTT Assay [b]	Stimulated PBMCs			-		
XTT Assay [b]	Monocyte-Macrophages			-		
XTT Assay [b]	Dendritic Cells			-		
XTT Assay [b]	Hepatocytes			-		
XTT Assay [b]	iPS Cardiomyocyte			-		
XTT Assay [b]	iPS Neurons			-		
XTT Assay [b]	RPTEC Kidney Cells			-		
GM Colony Formation [b]	Bone Marrow Progenitors					-
5 Day Toxicity Assay [a]	Rat Hepatocytes				-	
>80% Cell Loss [a]	HepG2	-		-		

AC50 Legend
++ = <0.2 μM
+ = 0.2-2 μM
+/- = 2-40 μM
- = >40 μM

[a]Data Generated through Cyprotex CellCiphr® Premier *in vitro* hepatotoxicity panel
http://www.cyprotex.com/toxicology/multiparametric/cellciphr-premier

[b]Data Generated through Imquest Toxi*SENS in vitro* toxicity panel
http://imquestbio.com/programs/in-vitro-toxicology/

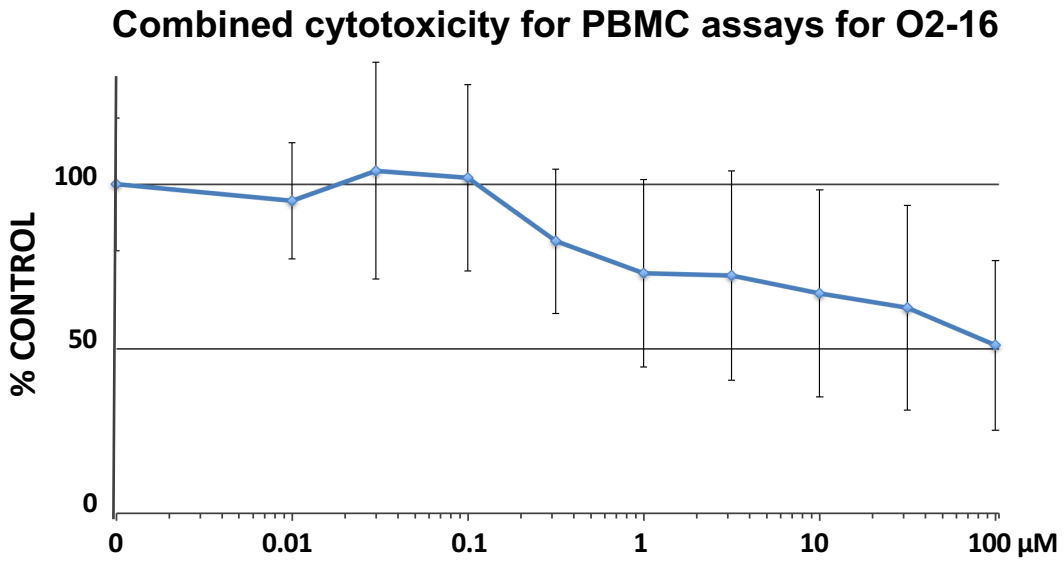

FIG. S6 related to FIG. 4. Combined cytotoxicity for PBMC assays for O2-16. All data points from tetrazolium based cell viability tests run in the PBMC assays were combined and cytotoxicity was calculated relative to 0 compound controls with error bars representing SD. The overall trend in the cytotoxicity profiles for O2-16 (n=12) was a gradual effect on cell viability consistent with cytostasis as opposed to overt cell toxicity consistent with the *in vitro* toxicity tests in Table S1.

TABLE S2. Alternative HIV Targets Tests: O2-16

Compound ID	Protease Assay[a] IC_{50}	Integrase Assay[b] IC_{50}	RT Biochem Assay[a] IC_{50}
O2-16	**> 100 µM**	**> 100 µM**	**> 100 µM**
Indinavir (PI)[c]	**30 nM**	> 10 µM	> 10 µM
Raltegravir (INI)[c]	ND[d]	**69 nM**	> 10 µM
AZT-TP (NRTI)[c]	ND[d]	ND[d]	**20 nM**
Nevirapine (NNRTI)[c]	ND[d]	ND[d]	**230 nM**

[a] Assay details are in Supplemental Materials and Methods (IC_{50}=50% Inhibitory Concentration)
[b] XpressBio HIV-1 Integrase Assay Kit was used according to manufacturer's protocol
[c] PI=Protease Inhibitor; INI=Integrase Inhibitor; NRTI=Nucleoside Reverse Transcription Inhibitor; NNRTI=Non-nucleoside Reverse Transcription Inhibitor
[d] ND=not determined

A. Time of Drug Addition Assay EC_{50} Values

Time of Addition Post-Infection (hr)	O2-16 (Vif Inhibitor)	Darunavir (Protease Inhibitor)	Maraviroc (Fusion Inhibitor)	AZT (NRTI)	Nevirapine (NNRTI)	Raltegravir (Integrase Inhibitor)	Temacrazine (RNA Trans. Inhibitor)
0	> 32.0	> 10.0	< 0.032	0.07	0.07	< 0.032	0.005
1	> 32.0	> 10.0	< 0.032	0.09	0.08	< 0.032	0.006
2	> 32.0	> 10.0	< 0.032	0.10	0.08	< 0.032	0.006
4	> 32.0	> 10.0	0.31	0.20	0.08	< 0.032	0.006
6	> 32.0	> 10.0	> 10.0	> 1.00	0.15	< 0.032	0.006
8	> 32.0	> 10.0	> 10.0	> 1.00	0.36	< 0.032	0.005
24	> 32.0	> 10.0	> 10.0	> 1.00	> 10.0	> 10.0	0.005

B

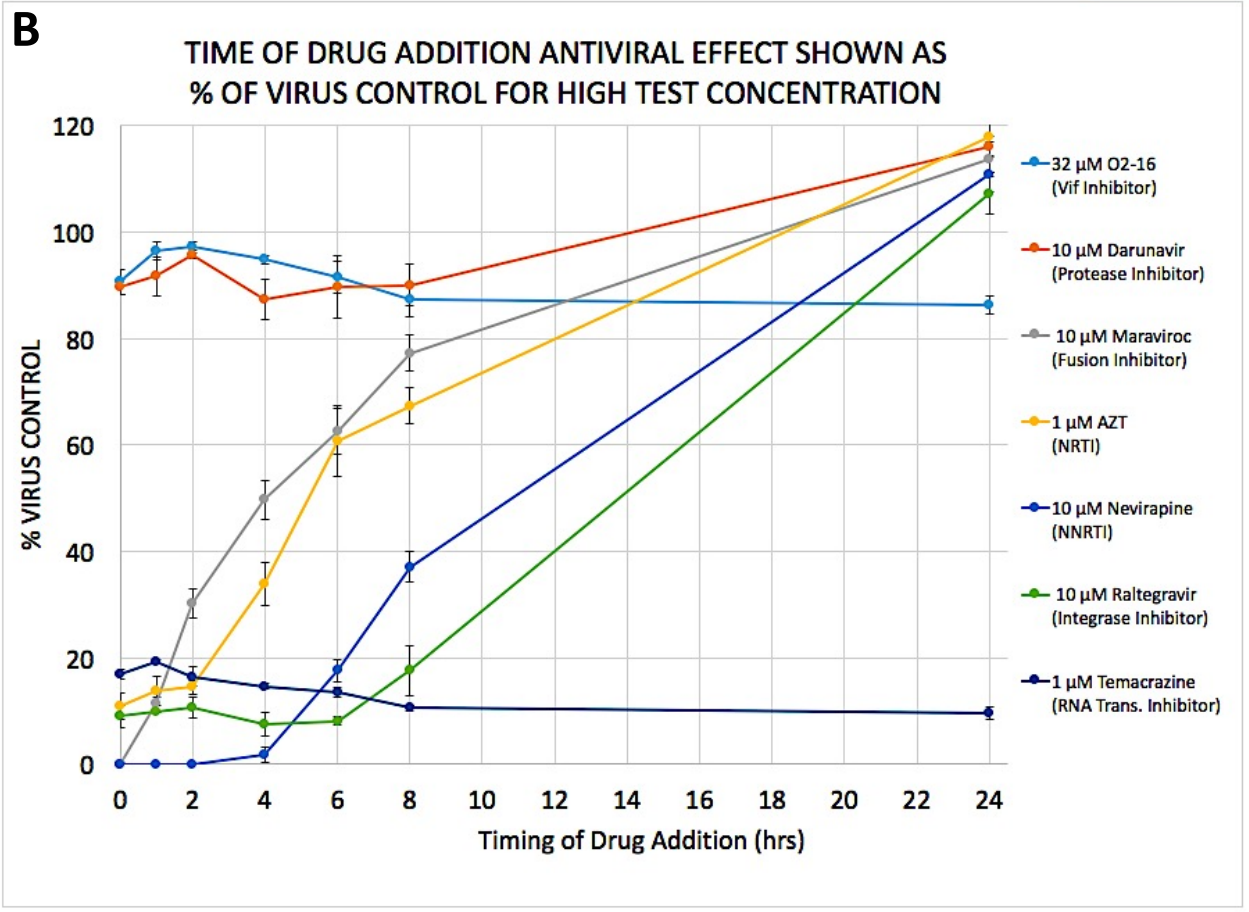

FIG. S7 related to FIG. 4. Time of Addition Assay in TZM-bl for O2-16. TZM-bl cells were infected with HIV Ba-L and each drug listed was added at 0, 1, 2, 4, 6, 8 and 24 hours after infection in triplicate. RLU values were measured 48 hrs post infection. Cytotoxicity tests were run side-by-side with the 0, 8, and 24 hr timepoints and none of the drugs showed significant toxicity at these timepoints. (A) Shows the EC_{50} values calculated from each 6-point dose curve with half-log doses down from the high test concentration for each drug (listed in B). (B) The graph shows the % infectivity for the high test concentration for each timepoint (drug concentrations listed on right) based on RLU values compared to RLU values from the no drug virus control cells, n=3 with error bars showing SD.

Supplemental Materials and Methods

Nested PCR and next generation sequencing (NGS)

885-bp amplicons from the *pol* gene of integrated proviruses or the vector control were amplified with Phusion DNA polymerase (Thermo) according to the manufacturer's protocol using outer primers 5-GCA CTT TAA ATT TTC CCA TTA GTC C-3 and 5-TGC AGA GCT AGA TGA ATT GCT TGT AAC-3. The relative amount of this outer amplicon was quantified with Quant-iT Picogreen (Thermo Fisher) according to manufacturer's protocol to normalize the amount of integrated provirus for the subsequent PCR. The second PCR was amplified with Phusion DNA polymerase using inner primers 5-GTA TAC TGC ATT TAC CAT ACC TAG TAT AAA C-3 and 5-GGA GGG GTA TTG ACA AAC T-3. Reaction conditions for both PCRs were as follows: 94 °C for 1 min; 25 cycles of the 83 °C for 30 s, 52 °C for 30 s, and 72 °C for 1 min; and a final extension at 72 °C for 5 min. PCR products run on agarose gels were visualized by ethidium bromide staining and isolated with the Wizard SV Gel and PCR Isolation Kit (Promega) according to manufacturer's protocol. The gel isolated PCR product was shipped to Edge Bio (Gaithersburg, MD) where NGS fragment libraries were generated for analysis with the Ion Torrent (Thermo Fisher) in order to quantify A3G signature hypermutations.

HIV-1 Protease Abz-Substrate Assay (Table S2)

Anthranilyl (Abz)-HIV Protease Substrate (Bachem H-2992) is a hexapeptide FRET substrate derived from the p24/p15 cleavage site of the viral gag-pol poly-protein, which allows the screening of potential HIV protease inhibitors. 1 mM Abz-Substrate was diluted with Assay Buffer to a working stock of 20 µM. A 50 µM stock HIV-1 protease (received from Sook-kyung Lee (UNC)) was diluted with Assay Buffer (50 mM HEPES, pH 6.8, 150 mM NaCl, and 1% DMSO) to a working stock of 100 nM. 2 µl 100 nM HIV-1 Protease along with 2 ul 20 µM Abz Substrate was added into each well and incubated at room temperature (avoiding light) for 1 hour before being read on an Envision plate reader (Perkin Elmer) excitation at 280 nm, emission at >435 nm.

HIV-1 RT Biochemical Assay (Table S2)

Purified recombinant HIV (pNL4-3) heterodimeric (p66/p51) Reverse Transcriptase (RT) was purchased from a commercially available source. The assay was performed in 96-well filter plate, where RT activity was determined by the incorporation of radiolabeled deoxyribonucleotides into the newly synthesized DNA strand. The RT reaction mixture

contained *in vitro* transcribed viral RNA derived from the HIV-1_{NL4-3} 5'-LTR region (position 454 to 652) and primer that is complementary to the primer binding site (PBS, nucleotide residues nucleotides 636 to 652), radiolabeled deoxyribonucleotide, dNTPs and reverse transcriptase. Briefly, the reaction was carried out in a volume of 50 µl containing 50 mM Tris HCl, pH 7.8, 50 mM KCl, 5mM $MgCl_2$, 1mM DTT, 50 µM each of dATP, dCTP, dGTP, 50 nM dTTP, 1µCi of [^{3}H] dTTP (70-90Ci/mM) and 5 nM template/primer. The reaction was initiated by the addition of 10 nM RT. For compound screening, serially diluted test articles were added to the reaction followed by the addition of RT. The reaction mixture was incubated at 37°C for 1h, and then quenched by the addition of ice-cold trichloroacetic acid (TCA) to the final concentration of 10%. The plate was incubated at 4°C for 1h to precipitate the synthesized DNA, then rinsed 3-times with 10% TCA and 1 time with 70% ethanol. After addition of 25 µl scintillation fluid to completely dried wells, radioactivity is counted by MicroBeta scintillation counter. The reduction of radioactivity represents the potency of compound inhibition.

Viral Isolates

The following virus isolates were obtained from the NIH AIDS Research and Reference Reagent Program, Division of AIDS, NIAID, NIH, as follows: HIV-1 group M isolates 92RW009 (subtype A; Cat# 1747), 92RW016 (subtype A; Cat# 2061), 98TZ013 (subtype C; Cat# 4171), 92UG021 (subtype D; Cat# 1648), 93UG067 (subtype D; Cat# 1953), 93BR020 (subtype F; Cat# 2329), and 92BR024 (subtype F/B; Cat# 1781) from the UNAIDS Network for HIV Isolation and Characterization (Gao et al., 1994); HIV-1 group M isolates 00KE_KER2008 (subtype A; Cat# 11242) and 98US_MSC5016 (subtype C; Cat# 11253) from Dr. Victoria Polonis (Brown et al., 2005); HIV-1 group M isolate IIIB (subtype B; Cat# 398) from Dr. Robert Gallo (Popovic et al., 1984; Ratner et al., 1985); HIV-1 group M isolate 92US159 (subtype B; Cat# 2761) from Dr. Cecelia Hutto; HIV-1 group M isolate QZ4589 (subtype B; Cat# 2258) from Drs. F. Cleghorn, C. Bartholomew, N. Jack, M. Greenberg, W. Blattner, and K. Weinhold; HIV-1 group M isolate 96USNG031 (subtype B; Cat# 4110) from Drs. D. Ellenberger, P. Sullivan, and R.B. Lal (Sullivan et al., 2000); HIV-1 group M isolates CMU02 (subtype E; Cat# 3023) and CMU08 (subtype E; Cat# 3025) from Dr. Kenrad Nelson; HIV-1 group M isolate JV1083 (subtype G; Cat# 3191) from Dr Alash'le Abimiku (Abimiku et al., 1994); HIV-1 group M isolate RU132 (subtype G; Cat# 3509) from Dr. A. Bobkov and Dr. Jonathon Weber; HIV-1 group O isolates BCF01 (Cat# 3333) and BCF02 (Cat# 3334), and group N isolate YBF30 (Cat# 4145) from Drs. Sentob Saragosti, Françoise Brun-Vézinet, and François Simon (Loussert-Ajaka

et al., 1995); NNRTI-resistant isolate A17 (Cat# 1413) from Dr. Emilio Emini (Nunberg et al., 1991); Enfuvirtide (T-20)-resistant isolate NL4-3 gp41 (36G) N42T, N43K (Cat# 9491) from Trimeris, Inc (Rimsky et al., 1998); Raltegravir-resistant isolates 4736_4 (Cat# 11842) and 8070_2 (Cat# 11845) from Dr. Robert Shafer and Elizabeth Reuman, M.S. (Reuman et al., 2010); and HIV-1 molecular clone pNL4-3 from Dr. Malcolm Martin (Adachi et al., 1986). In addition, the multidrug-resistant HIV-1 clinical isolates MDR769 and MDR807 were obtained from Dr. Thomas C. Merigan of Stanford University (Palmer et al., 1999), and the Protease Inhibitor (PI)-resistant HIV-1 clinical isolate 1022-48 was obtained from Dr. William A. Schleif of Merck Research Laboratories (contains Protease mutations L10I, T12S, I13V, L33I, M36I, M46I, I64V, V82F, I84V, and L89M).

Supplemental References

Abimiku, A.G., Stern, T.L., Zwandor, A., Markham, P.D., Calef, C., Kyari, S., Saxinger, W.C., Gallo, R.C., Robert-Guroff, M., Reitz, M.S., 1994. Subgroup G HIV type 1 isolates from Nigeria. AIDS Res Hum Retroviruses 10, 1581-1583.

Adachi, A., Gendelman, H.E., Koenig, S., Folks, T., Willey, R., Rabson, A., Martin, M.A., 1986. Production of acquired immunodeficiency syndrome-associated retrovirus in human and nonhuman cells transfected with an infectious molecular clone. J Virol 59, 284-291.

Brown, B.K., Darden, J.M., Tovanabutra, S., Oblander, T., Frost, J., Sanders-Buell, E., de Souza, M.S., Birx, D.L., McCutchan, F.E., Polonis, V.R., 2005. Biologic and genetic characterization of a panel of 60 human immunodeficiency virus type 1 isolates, representing clades A, B, C, D, CRF01_AE, and CRF02_AG, for the development and assessment of candidate vaccines. J Virol 79, 6089-6101.

Ganesan, S., Ameer-Beg, S.M., Ng, T.T., Vojnovic, B., Wouters, F.S., 2006. A dark yellow fluorescent protein (YFP)-based Resonance Energy-Accepting Chromoprotein (REACh) for Forster resonance energy transfer with GFP. Proc Natl Acad Sci U S A 103, 4089-4094.

Gao, F., Yue, L., Craig, S., Thornton, C.L., Robertson, D.L., McCutchan, F.E., Bradac, J.A., Sharp, P.M., Hahn, B.H., 1994. Genetic variation of HIV type 1 in four World Health Organization-sponsored vaccine evaluation sites: generation of functional envelope (glycoprotein 160) clones representative of sequence subtypes A, B, C, and E. WHO Network for HIV Isolation and Characterization. AIDS Res Hum Retroviruses 10, 1359-1368.

Loussert-Ajaka, I., Chaix, M.L., Korber, B., Letourneur, F., Gomas, E., Allen, E., Ly, T.D., Brun-Vezinet, F., Simon, F., Saragosti, S., 1995. Variability of human immunodeficiency virus type 1 group O strains isolated from Cameroonian patients living in France. J Virol 69, 5640-5649.

Nunberg, J.H., Schleif, W.A., Boots, E.J., O'Brien, J.A., Quintero, J.C., Hoffman, J.M., Emini, E.A., Goldman, M.E., 1991. Viral resistance to human immunodeficiency virus type 1-specific pyridinone reverse transcriptase inhibitors. J Virol 65, 4887-4892.

Palmer, S., Shafer, R.W., Merigan, T.C., 1999. Highly drug-resistant HIV-1 clinical isolates are cross-resistant to many antiretroviral compounds in current clinical development. AIDS 13, 661-667.

Popovic, M., Sarngadharan, M.G., Read, E., Gallo, R.C., 1984. Detection, isolation, and continuous production of cytopathic retroviruses (HTLV-III) from patients with AIDS and pre-AIDS. Science 224, 497-500.

Ratner, L., Haseltine, W., Patarca, R., Livak, K.J., Starcich, B., Josephs, S.F., Doran, E.R., Rafalski, J.A., Whitehorn, E.A., Baumeister, K., et al., 1985. Complete nucleotide sequence of the AIDS virus, HTLV-III. Nature 313, 277-284.

Reuman, E.C., Bachmann, M.H., Varghese, V., Fessel, W.J., Shafer, R.W., 2010. Panel of prototypical raltegravir-resistant infectious molecular clones in a novel integrase-deleted cloning vector. Antimicrob Agents Chemother 54, 934-936.

Rimsky, L.T., Shugars, D.C., Matthews, T.J., 1998. Determinants of human immunodeficiency virus type 1 resistance to gp41-derived inhibitory peptides. J Virol 72, 986-993.

Sullivan, P.S., Do, A.N., Ellenberger, D., Pau, C.P., Paul, S., Robbins, K., Kalish, M., Storck, C., Schable, C.A., Wise, H., Tetteh, C., Jones, J.L., McFarland, J., Yang, C., Lal, R.B., Ward, J.W., 2000. Human immunodeficiency virus (HIV) subtype surveillance of African-born persons at risk for group O and group N HIV infections in the United States. J Infect Dis 181, 463-469.